Liu *et al.*
European Journal of Medical Research (2025) 30:149
https://doi.org/10.1186/s40001-025-02407-8

European Journal of Medical Research

RESEARCH

Open Access

Expression patterns of MCM8 in lung adenocarcinoma and its correlation with key biological processes

Xu-Sheng Liu[2,3,4*†], Jin Xie[5†], Rui-Min Wu[2], Gao-Chun Xiao[6], Yu Zhang[2] and Zhi-Jun Pei[1*]

Abstract

Objective Lung adenocarcinoma (LUAD) is one of the most common and lethal tumors. The identification of diagnostic and prognostic biomarkers is essential to improve patient prognosis and treatment outcomes.

Methods The expression of minichromosome maintenance complex component 8 (MCM8) in 33 cancer types was analyzed using the Cancer Genome Atlas (TCGA) and Genotype-Tissue Expression. Tumor and normal tissues in LUAD were compared using TCGA data and validated against four datasets from the Gene Expression Omnibus. MCM8 expression was assessed by immunohistochemistry (IHC) using tissue microarrays. The diagnostic value of MCM8 was assessed by Receiver Operating Characteristic curve analysis, and its prognostic significance was determined by Kaplan–Meier analysis. The CIBERSORT method was used to examine immune infiltration. The association between MCM8 expression and m6A RNA methylation, glycolysis, and ferroptosis was assessed using the GEPIA online tool.

Results MCM8 is markedly overexpressed in many tumors including LUAD. MCM8 showed high accuracy for the diagnosis of LUAD, with an area under the curve of 0.849 in TCGA dataset. MCM8 overexpression in tumor tissues in LUAD was confirmed by IHC and shown to be associated with decreased overall survival and disease-specific survival. Analysis of immune cell infiltration showed that immune cell populations differed between high and low MCM8 expression groups. MCM8 expression correlated with that of genes associated with m6A RNA methylation, glycolysis, and ferroptosis.

Conclusions MCM8 was identified as a promising diagnostic and prognostic marker in LUAD. The mechanism underlying the effect of MCM8 on cancer development and the immune response remains to be elucidated.

Keywords MCM8, Lung adenocarcinoma, m6A, Glycolysis, Ferroptosis, Immune infiltration

†Xu-Sheng Liu and Jin Xie have contributed equally to this work.

*Correspondence:
Xu-Sheng Liu
lxsking@taihehospital.com
Zhi-Jun Pei
pzjzml1980@taihehospital.com
[1] Department of Nuclear Medicine, The Second Affiliated Hospital of Soochow University, Suzhou 215004, Jiangsu, China
[2] Department of Nuclear Medicine, Hubei Provincial Clinical Research Center for Precision Diagnosis and Treatment of Liver Cancer, Taihe Hospital, Hubei University of Medicine, Shiyan 442000, Hubei, China
[3] Hubei Provincial Clinical Research Center for Umbilical Cord Blood Hematopoietic Stem Cells, Taihe Hospital, Hubei University of Medicine, Shiyan 442000, Hubei, China
[4] Hubei Key Laboratory of Embryonic Stem Cell Research, Shiyan 442000, Hubei, China
[5] Hubei University of Traditional Chinese Medicine, Wuhan 430065, Hubei, China
[6] Department of General Surgery, Taihe Hospital, Hubei University of Medicine, Shiyan 442000, Hubei, China

Introduction

Lung adenocarcinoma (LUAD) is a common and deadly subtype of lung cancer, and its incidence is increasing worldwide. In the United States, lung cancer is the leading cause of cancer-related mortality, accounting for 21% of all cancer-related deaths [1]. Despite advances in surgical techniques, chemotherapy, and targeted therapies, the 5-year survival rate of patients with LUAD remains dismally low, hovering around 25% [1, 2], underscoring the need to identify novel diagnostic markers and therapeutic targets to improve patient outcomes [3–5].

The current standard treatments for LUAD, including surgery, radiotherapy, and chemotherapy, have considerable limitations. Surgical resection is often not feasible for advanced-stage patients, and chemotherapeutic regimens are frequently associated with severe side effects and the development of resistance [6, 7]. Targeted therapies such as epidermal growth factor receptor (EGFR) inhibitors have shown promise, but are limited by the development of resistance and the heterogeneity of tumor biology [8, 9]. Immunotherapy has emerged as a new frontier in cancer treatment; however, its efficacy is limited to a subset of patients, and novel biomarkers capable of predicting the response to therapy need to be identified to guide the design of treatment strategies [10–15].

Minichromosome maintenance complex component 8 (MCM8) functions in DNA replication and repair, and it is dysregulated in various cancers. MCM8 is overexpressed in many tumors [16–20] and is considered a potential biomarker for cancer diagnosis and prognosis because of its role in cell proliferation and genomic stability [21, 22]. However, the role of MCM8 in LUAD remains underexplored, making it a promising candidate for further investigation.

The aim of this study was to determine the diagnostic and prognostic value of MCM8 in LUAD. We examined the expression profiles of MCM8 in 33 distinct tumor types using data derived from The Cancer Genome Atlas (TCGA) and the Genotype-Tissue Expression (GTEx) projects. MCM8 expression was compared between LUAD and normal lung tissues, and the findings were validated using four independent Gene Expression Omnibus (GEO) datasets. The diagnostic accuracy of MCM8 was determined by Receiver Operating Characteristic (ROC) analysis, and its prognostic significance was assessed using survival data from TCGA LUAD cohort. The relationship between MCM8 expression and immune cell infiltration in LUAD was examined using the CIBERSORT algorithm and Spearman correlation analysis. We found an association between MCM8 and key biological processes such as N6-methyladenosine (m6A) RNA methylation, glycolysis, and ferroptosis, which provides valuable information on its broader implications in LUAD pathology. The current findings suggest that MCM8 could serve as a biomarker for early diagnosis and a prognostic indicator, as well as a target for therapeutic intervention, thereby offering new avenues for improving patient management in LUAD.

Materials and methods

Comprehensive analysis of MCM8 expression in pan-cancer studies

To determine the potential role of MCM8 in oncogenesis, we analyzed its expression in 33 different tumor types using the TCGA and GTEx pan-cancer datasets sourced from the UCSC XENA platform (https://xenabrowser.net/datapages/, accessed on May 20, 2024), which include RNA sequencing data. The expression of MCM8 was compared between tumor and normal tissues by analyzing data from TCGA LUAD dataset (https://portal.gdc.cancer.gov, accessed on 20 May 2024) [23]. Differences in MCM8 expression between LUAD and normal samples were confirmed in four LUAD datasets from the GEO (https://www.ncbi.nlm.nih.gov/geo/, accessed on 20 May 2024) repository, specifically GSE32036, GSE27262, GSE31210, and GSE40791.

Prognostic and diagnostic evaluation of MCM8 in LUAD

The relationship between MCM8 expression and the clinicopathological characteristics of patients with LUAD was analyzed to determine the potential of MCM8 as a diagnostic marker. ROC analysis was performed using the pROC package in R with default parameters for curve generation and AUC estimation; the 95% confidence interval (CI) was calculated through bootstrapping [24]. The outcomes of the analysis were visualized using the ggplot2 package, which provides a comprehensive visual overview of the diagnostic value of MCM8. Kaplan–Meier survival analysis was performed using the BEST online tool (https://rookieutopia.hiplot.com.cn/app_direct/BEST/, accessed on 21 May 2024) [25]. Patients were stratified into high and low MCM8 expression groups based on the median expression value. Survival differences between the groups were assessed using the log-rank test, and hazard ratios (HRs) with 95% CIs were calculated using the Cox proportional hazards model. We performed a Cox proportional hazard analysis to further investigate the impact of MCM8 expression on survival outcomes in patients from TCGA LUAD. Specifically, we included T stage, N stage, M stage, and MCM8 expression in our analysis.

Tissue microarray (TMA)

TMA slides were purchased from Zhuoli Biotechnology Co., Ltd. (ZL-LugA961, Shanghai, China). The TMA contained 48 cases, including both LUAD tissues and their

paired normal tissues (paracancerous tissues), arranged in duplicate for each case.

Immunohistochemistry (IHC)

The expression of the MCM8 protein in LUAD and adjacent normal tissues was evaluated by IHC using rabbit anti-MCM8 polyclonal antibody (Beijing Bioss Biotechnology Co., Ltd.) at a dilution of 1:100. The sections were incubated with the primary antibody overnight at 4 °C in a humidified chamber. After three washes with PBS, the section were incubated with horseradish peroxidase-conjugated secondary antibody for 30 min at room temperature. Color development was performed with a diaminobenzidine (DAB) substrate, followed by counterstaining with hematoxylin. After dehydration and clearing, the sections were mounted for microscopic examination [26].

Semi-quantitative image analysis

After staining, the slides were scanned, and digital images were captured using a light microscope equipped with a digital camera. Semi-quantitative assessment of MCM8 expression was performed using ImageJ software (National Institutes of Health, Bethesda, MD, USA). The percentage of positively stained areas (%Area) was calculated for each image to quantify MCM8 expression. The analysis was performed for all 48 tumor tissues and their paired paracancerous tissues to compare MCM8 protein expression between the two groups.

Immune infiltration in LUAD according to MCM8 expression

To explore the immunological significance of MCM8 expression in LUAD, we divided the TCGA LUAD dataset into two groups according to MCM8 expression: a high-expression group and a low-expression group. The CIBERSORT core algorithm [27] and the markers for 22 immune cell types provided by the CIBERSORTx website (https://cibersortx.stanford.edu/, accessed on 23 May 2024) [28] were used to obtain immune infiltration profiles for each group. Box plots were generated to analyze the differences in immune cells between the two MCM8 expression groups. The relationship between the expression of MCM8 and the amounts of the 22 immune cell types was analyzed using Spearman's rank correlation.

Correlation of MCM8 expression with key biological processes in LUAD

The correlation analysis module of the Gene Expression Profiling Interactive Analysis (GEPIA) online database (http://GEPIA.cancer-pku.cn/#correlation, accessed on 24 May 2024) [29] was used to examine the association of MCM8 expression with biological processes in LUAD, with particular emphasis on m6A RNA methylation, glycolysis, and ferroptosis. The gene lists for these processes were curated as described previously [30–35]. Pearson's correlation analysis of three distinct datasets, TCGA LUAD, GSE31210, and GSE40791, was performed to quantify the correlation between MCM8 expression levels and genes implicated in m6A modification, glycolysis, and ferroptosis in LUAD. This comprehensive assessment aimed to uncover potential associations between MCM8 expression and these vital biological pathways, thereby shedding light on novel insights into LUAD pathogenesis. We identified genes that consistently exhibited significant correlations across all three datasets, reinforcing the robustness of our observations. The associations between MCM8 expression and the biological processes were evaluated using Pearson correlation analysis. The expression levels of genes linked to m6A modification, glycolysis, and ferroptosis were compared between MCM8 high- and low-expression groups.

Statistics analysis

Statistical analyses were performed using the R software package using established statistical methodologies. To enhance the interpretability and impact of our discoveries, we employed the Xiantao Online Tool (https://www.xiantaozi.com/, accessed on 20 May 2024) for data visualization. This platform's intuitive interface and comprehensive functionality allowed us to create clear and informative visualizations that effectively communicated the patterns and trends within our data. A threshold of $P < 0.05$ was considered statistically significant.

Results

Pan-cancer expression profiling of MCM8

MCM8 expression in different cancer types was examined using TCGA and GTEx datasets. MCM8 was significantly upregulated in bladder urothelial carcinoma, breast invasive carcinoma, cervical squamous cell carcinoma and endocervical adenocarcinoma, cholangiocarcinoma, colon adenocarcinoma, lymphoid neoplasm diffuse large B-cell lymphoma, esophageal carcinoma, glioblastoma multiforme, head and neck squamous cell carcinoma, brain lower grade glioma, liver hepatocellular carcinoma, LUAD, lung squamous cell carcinoma, ovarian serous cystadenocarcinoma, pancreatic adenocarcinoma, rectum adenocarcinoma, skin cutaneous melanoma, stomach adenocarcinoma, thymoma, and uterine carcinosarcoma compared with normal tissues (Fig. 1A, $P < 0.05$). MCM8 expression was downregulated in kidney renal clear cell carcinoma, acute myeloid leukemia, prostate adenocarcinoma, testicular germ cell tumors, and thyroid carcinoma. Fig. 1B shows that the expression level of MCM8 in tumor samples

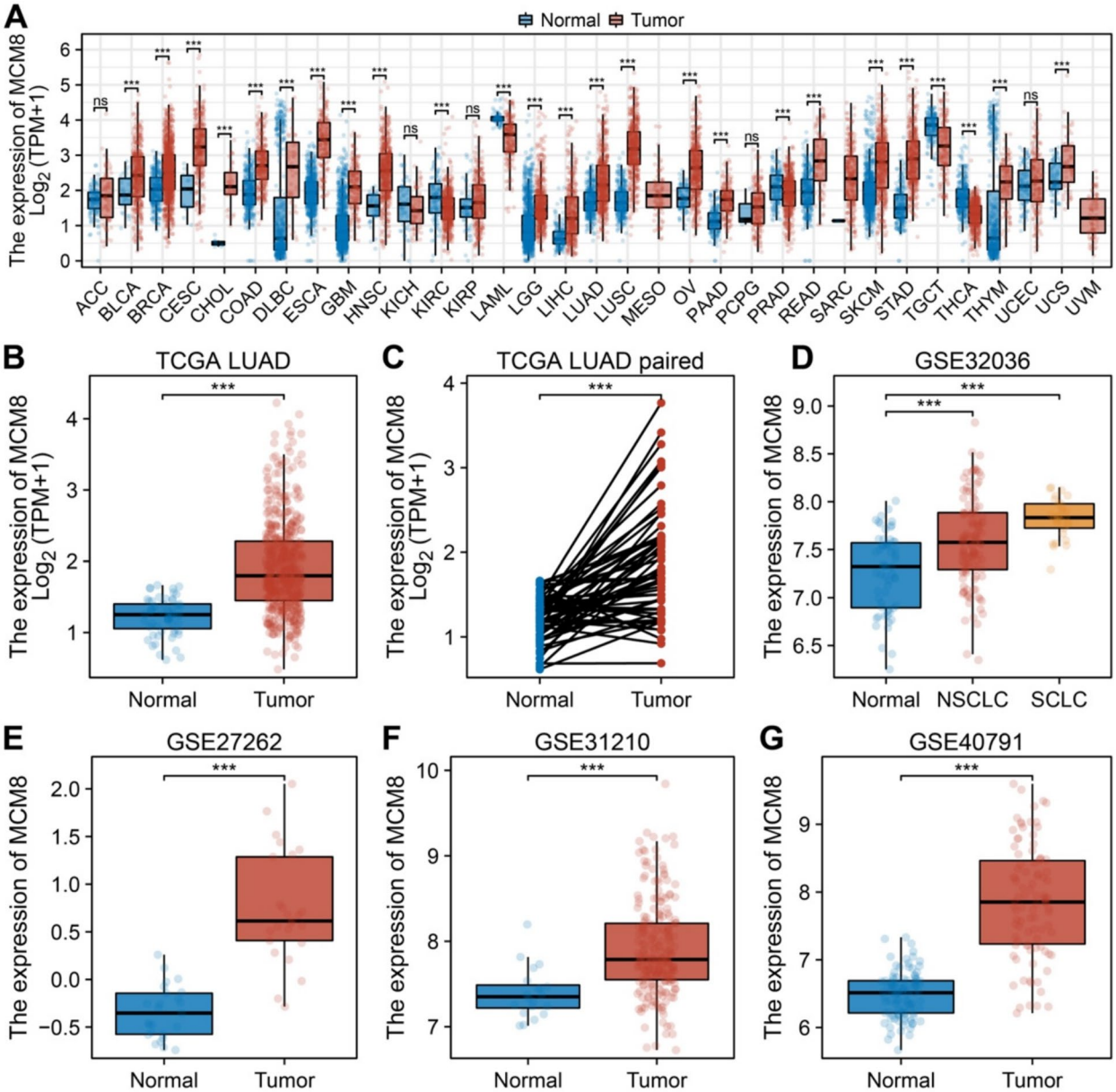

Fig. 1 Pan-Cancer Analysis of MCM8 Expression. **A** Analysis of TCGA And GTEx data showed that MCM8 expression was higher in cancer than in normal tissues (P < 0.05). **B** The expression level of MCM8 in tumor samples was significantly higher than that in normal samples (P <0.05). **C** Plot showing elevated MCM8 expression in TCGA LUAD dataset relative to matched normal control samples (P < 0.05). **D**–**G** Statistical analysis showed increased MCM8 expression in LUAD samples compared with control groups from the GSE32036, GSE27262, GSE31210, and GSE40791 datasets (P < 0.05)

from the TCGA LUAD dataset was significantly higher than in normal samples (P < 0.05). MCM8 expression was significantly higher in TCGA LUAD samples than in the corresponding control samples (Fig. 1C, P < 0.05). Analysis of the GSE32036, GSE27262, GSE31210, and GSE40791 datasets confirmed that MCM8 expression was higher in LUAD samples than in the controls (Fig. 1D–G, P < 0.05).

Assessment of MCM8 expression patterns and clinical relevance in LUAD Patients

To examine the possible clinical implications of MCM8, we analyzed patient data from TCGA focusing on LUAD specimens. We found that MCM8 levels were higher in malignant tissue samples from all disease stages (I, II, III, and IV) than in their normal counterparts (Fig. 2A, P < 0.05). Analysis according to tumor (T) stage showed

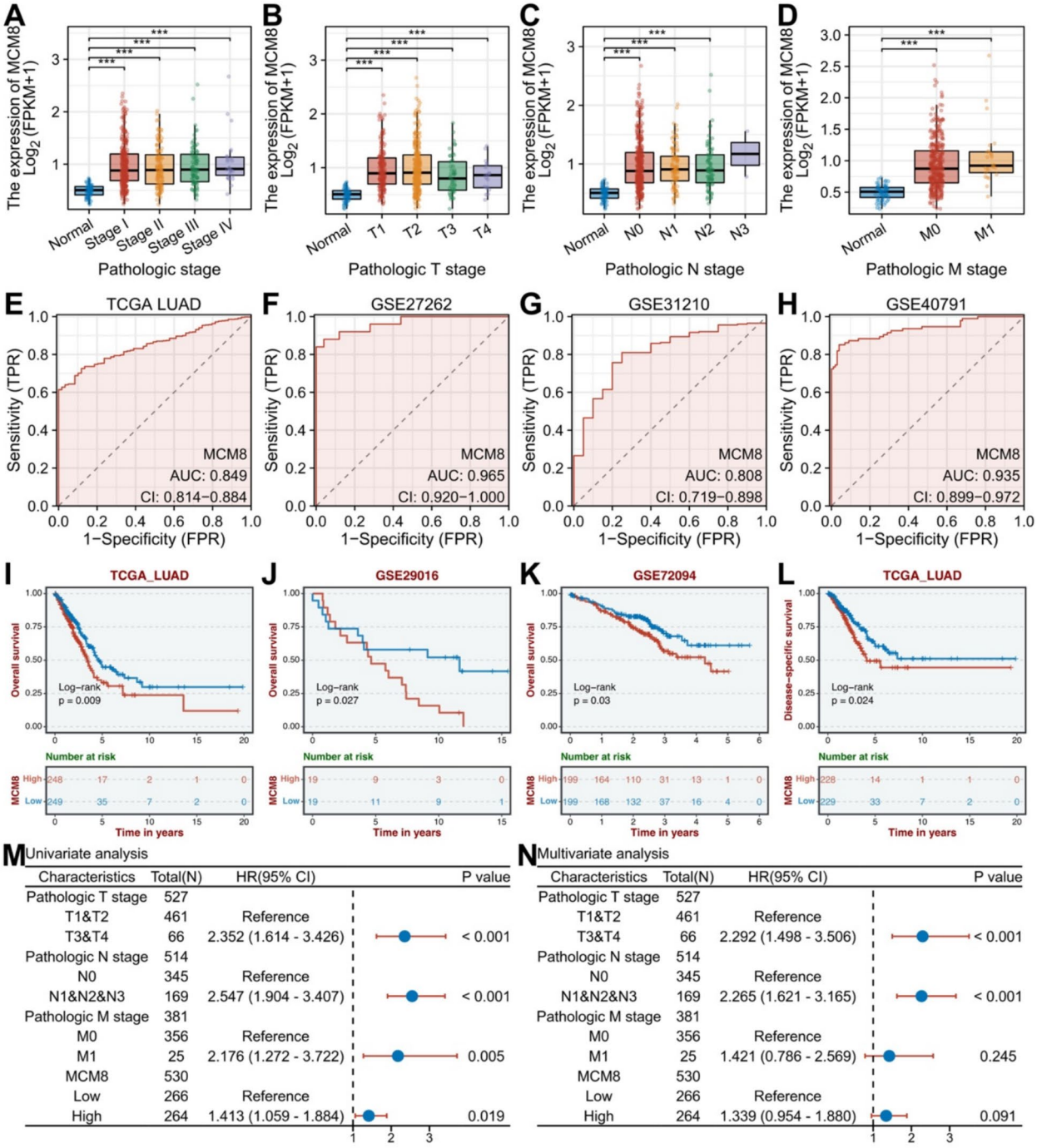

Fig. 2 Assessment of MCM8 Expression Patterns and Clinical Relevance in LUAD Patients. **A** Box plot showing significantly elevated MCM8 expression in tumor samples from all stages (I, II, III, and IV) compared with normal tissues ($P < 0.05$). **B**–**D** Box plots showing consistently higher MCM8 expression in tumor samples at T1, T2, T3, T4 stages **B**, N0, N1, N2 stages **C**, and M0, M1 stages (**D**) than in normal tissues ($P < 0.05$). **E**–**H** ROC curves demonstrating the potential of MCM8 for predicting LUAD accurately, as indicated by AUC values for TCGA LUAD (**E**), GSE27262 (**F**), GSE31210 (**G**), and GSE40791 (**H**). **I**–**K** Kaplan–Meier survival curves indicating that high MCM8 expression is associated with poor overall survival (OS) in the TCGA LUAD, GSE29016, and GSE72094 datasets ($P < 0.05$). **L** Kaplan–Meier survival curve showing that high MCM8 expression is associated with poor disease-specific survival (DSS) in TCGA LUAD dataset ($P < 0.05$). **M** Univariate Cox analysis. **N** Multivariate Cox analysis

that MCM8 levels were higher in cancerous tissues at T1, T2, T3, and T4 stages than in non-cancerous tissues (Fig. 2B, P < 0.05), and similar results were obtained according to node (N) stage, with MCM8 levels higher in N0, N1, and N2 stages than in normal tissues (Fig. 2C, P < 0.05). MCM8 levels were also elevated in tumor samples from M0 and M1 stages than in non-malignant samples (Fig. 2D, P < 0.05). These observations collectively suggest an association between MCM8 expression and the progression of LUAD. The efficacy of MCM8 as a diagnostic marker for LUAD was assessed by ROC curve analysis, which indicated that MCM8 could accurately predict LUAD, with AUC values of 0.849 (95% CI 0.814–0.884) in TCGA LUAD (Fig. 2E), 0.965 (95% CI 0.920–1.000) in GSE27262 (Fig. 2F), 0.808 (95% CI 0.719–0.898) in GSE31210 (Fig. 2G), and 0.935 (95% CI 0.899–0.972) in GSE40791 (Fig. 2H). The prognostic significance of MCM8 expression was assessed by Kaplan–Meier survival analysis. The results showed that elevated MCM8 expression was associated with poor overall survival (OS) in TCGA LUAD, GSE29016, and GSE72094 datasets (Fig. 2I–K, P < 0.05). In TCGA LUAD dataset, MCM8 upregulation was also associated with poor disease-specific survival (DSS) (Fig. 2L, P < 0.05). Univariate Cox analysis showed that T stage, N stage, M stage, and MCM8 expression were significantly associated with prognosis (Fig. 2M, P < 0.05). However, in the multivariate Cox analysis, only T stage and N stage maintained statistically significant associations (Fig. 2N, P < 0.05).

MCM8 overexpression in LUAD tissues

Next, the expression of MCM8 in tissue microarray (TMA) chips from LUAD patients was examined by IHC staining. Representative IHC images of tumors and paired adjacent non-cancerous tissues from LUAD patients, as well as the histological grading of tumor patients, are shown in Fig. 3A. The results of semi-quantitative analysis indicated that MCM8 was significantly overexpressed in LUAD tissue samples compared with adjacent non-cancerous tissues (Fig. 3B, P < 0.05). MCM8 expression was significantly higher in different histological grades (Grades II and III), ACJJ stages (I, II), T stages (T1, T2), N stages (N0), and M Stage (M0) compared with adjacent non-cancerous tissues (Fig. 3E–I, P < 0.05). The expression of MCM8 was not related to age or gender (Fig. 3C, D, P > 0.05). Groups with fewer than three samples were not included in the statistical analysis.

Immune infiltration analysis in LUAD Based on MCM8 expression

The CIBERSORT algorithm was used to measure the proportion of infiltrating immune cells in the high and low MCM8 expression groups in TCGA LUAD dataset (Fig. 4A). The results indicated that samples with high MCM8 expression had significantly elevated levels of infiltration of T cells CD4 memory activated (P = 7.7e-09), NK cells resting (P = 7.9e-06), macrophages M0 (P = 0.0012), and macrophages M1 (P = 1.63e-05), whereas those with low MCM8 expression had higher infiltration levels of plasma cells (P = 0.0059), T cells regulatory [Tregs] (P = 0.0233), NK cells activated (P = 3.03e-05), monocytes (P = 0.0475), dendritic cells resting (P = 0.0001), and mast cells resting (P = 2.14e-06) (Fig. 4B). Correlation analysis showed that in the TCGA LUAD dataset, MCM8 expression was negatively correlated with mast cells resting (Cor = -0.231, P = 5.59E-08), dendritic cells resting (Cor = − 0.208, P = 1.05E-06), NK cells activated (Cor = − 0.152, P = 4.00E-04), plasma cells (Cor = − 0.130, P = 2.50E-03), Tregs (Cor = − 0.115, P = 7.70E-03), neutrophils (Cor = − 0.113, P = 8.80E-03), monocytes (Cor = − 0.102, P = 1.78E-02), and T cells gamma delta (Cor = − 0.088, P = 4.10E-02) (Fig. 4C). MCM8 was positively correlated with macrophages M0 (Cor = 0.146, P = 7.00E-04), NK cells resting (Cor = 0.195, P = 5.11E-06), macrophages M1 (Cor = 0.225, P = 1.37E-07), and T cells CD4 memory activated (Cor = 0.236, P = 2.86E-08).

MCM8 expression and its potential interaction with the m6A methylation machinery in LUAD

The potential association between MCM8 expression and genes involved in m6A methylation in LUAD was examined using the GEPIA online tool. A positive correlation between the expression levels of MCM8 and a set of 20 genes associated with m6A modification was identified (Fig. 5A, R = 0.69, P = 6.7e-69). Analysis of TCGA LUAD dataset confirmed the positive association between MCM8 and m6A-modifying genes (Fig. 5B, P < 0.05). In the GSE31210 dataset, MCM8 expression was significantly positively associated with HNRNPA2B1, IGF2BP1, IGF2BP2, IGF2BP3, RBM15, VIRMA, YTHDF1, and YTHDF3, and significantly negatively associated with FTO, METTL14, and YTHDC1 (Fig. 5B, P < 0.05). In the GSE40791 dataset, MCM8 expression was positively associated with multiple genes, including HNRNPA2B1, IGF2BP1, IGF2BP2, METTL3, RBM15, VIRMA, YTHDC2, and YTHDF1. Conversely, an inverse relationship was noted with ALKBH5 (Fig. 5B, P < 0.05). The significant positive correlation between MCM8 and the m6A genes HNRNPA2B1, IGF2BP1, IGF2BP2, RBM15, VIRMA, and YTHDF1 in the three datasets was visualized using scatter plots (Fig. 5C, P < 0.05).

Further exploration of TCGA LUAD dataset identified 19 m6A genes whose expression differed significantly between high- and low-MCM8 expression groups, including FTO, HNRNPA2B1, HNRNPC, IGF2BP1,

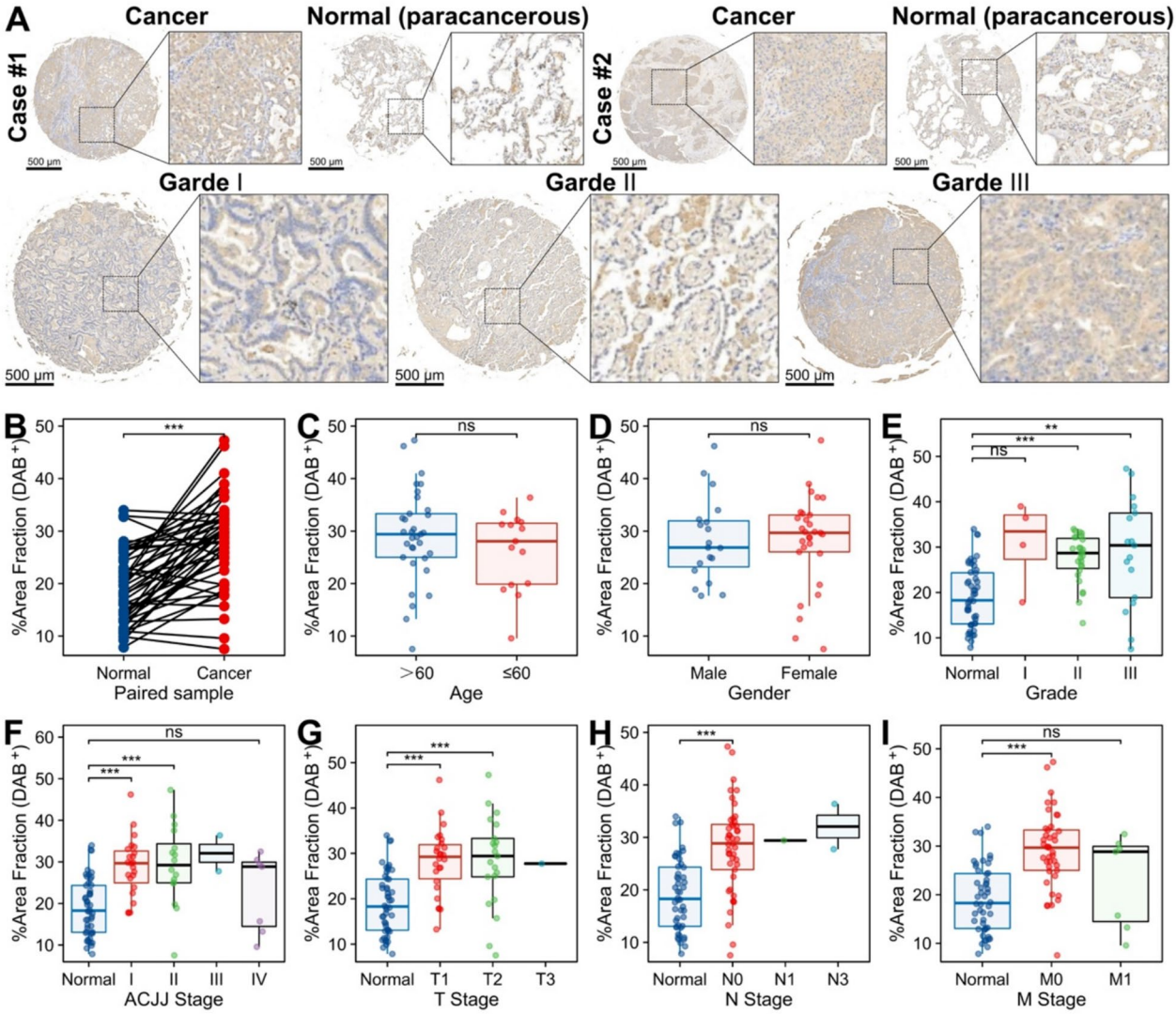

Fig. 3 Expression of MCM8 in LUAD Tissue Microarrays. **A** Representative immunohistochemistry (IHC) staining images of LUAD tumor tissues and paired adjacent non-cancerous tissues. **B** Semi-quantitative analysis showing significantly higher MCM8 expression in LUAD than in adjacent non-cancerous tissues ($P < 0.05$). **C**, **D** MCM8 expression was not significantly associated with patient age or gender ($P > 0.05$). **E**–**I** MCM8 expression was significantly elevated in different histological grades, ACJJ stages, and T, N, and M stages ($P < 0.05$)

IGF2BP2, IGF2BP3, METTL14, METTL3, RBM15, RBM15B, RBMX, VIRMA, WTAP, YTHDC1, YTHDC2, YTHDF1, YTHDF2, YTHDF3, and ZC3H13 (Fig. 5D, $P < 0.05$). A Venn diagram was generated to show that HNRNPA2B1, IGF2BP1, IGF2BP2, RBM15, VIRMA, and YTHDF1 met the criteria of all four analyses, suggesting a potential linkage with MCM8 (Fig. 5E).

Association between MCM8 expression and glycolysis in LUAD

The association between MCM8 expression and glycolysis in LUAD was analyzed using the GEPIA online tool. We found a significant positive correlation between MCM8 expression and a panel of 11 glycolysis-related genes (Fig. 6A, $R = 0.46$, $P = 2e\text{-}28$). This observation suggests that MCM8 is involved in the regulation of the glycolysis pathway in LUAD cells. To validate this association, we analyzed TCGA LUAD dataset and observed a consistent positive correlation between MCM8 and nine of the glycolysis genes, namely SLC2A1, HK2, GPI, ALDOA, GAPDH, PGK1, PGAM1, ENO1, and LDHA (Fig. 6B, $P < 0.05$). This correlation was also evident in two additional datasets, GSE31210 and GSE40791, further supporting the potential linkage between MCM8 and glycolysis in LUAD. MCM8 expression was significantly positively correlated with 11 glycolysis genes in

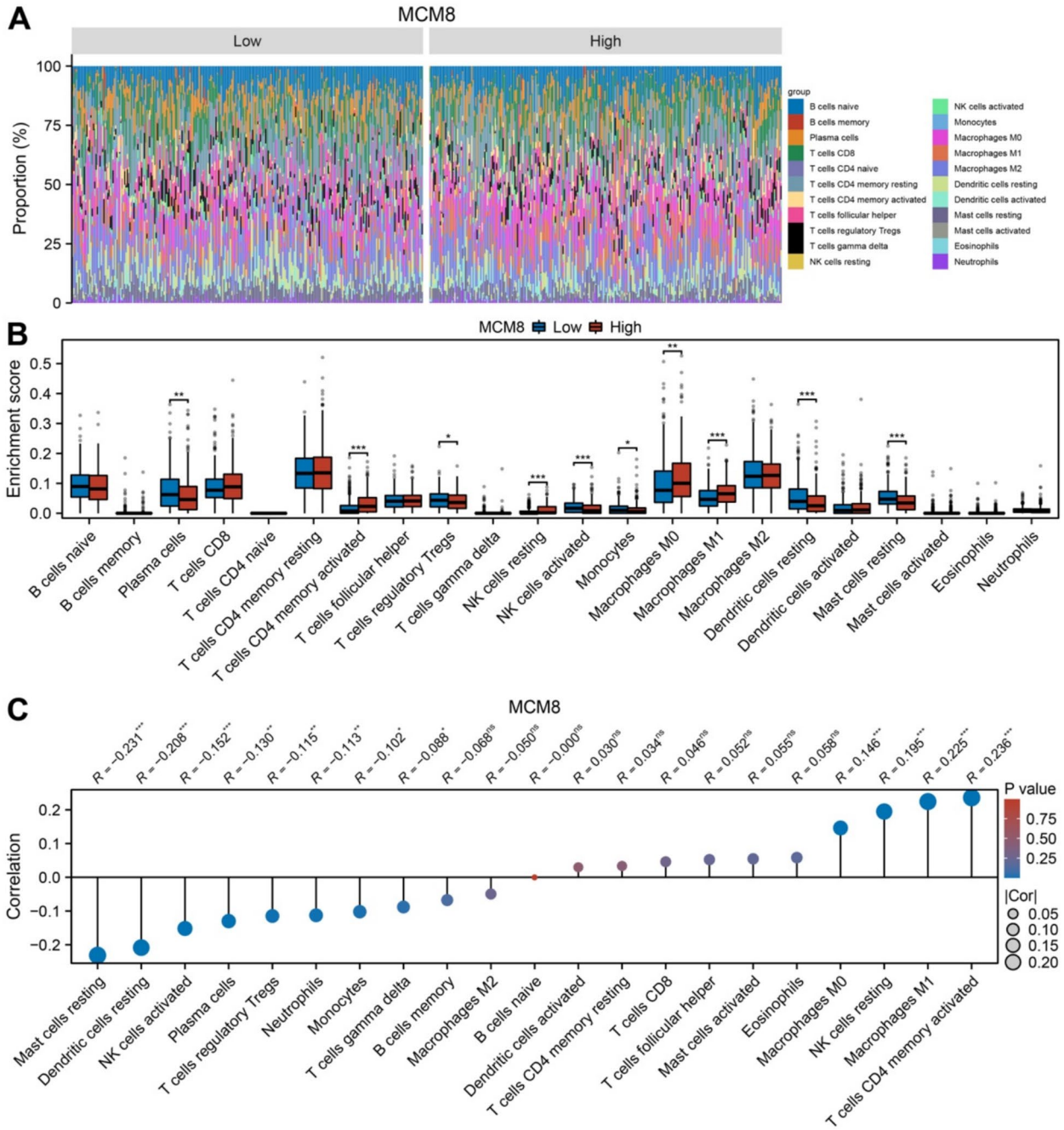

Fig. 4 Immune Cell Infiltration Patterns and Their Association with MCM8 Expression in TCGA LUAD Dataset. **A** The relative proportions of infiltrated immune cells were determined by the CIBERSORT algorithm in high- and low-MCM8 expression groups in TCGA LUAD dataset. **B** Comparative analysis of immune cell infiltration levels in high- and low-MCM8 expression groups, emphasizing notable differences. **C** Correlation analysis showing the association between MCM8 expression and different immune cell types in TCGA LUAD dataset

the GSE31210 dataset, whereas in the GSE40791 dataset, it was positively correlated with GPI, GAPDH, PGAM1, ENO1, and LDHA (Fig. 6B, $P < 0.05$). Figure 6C shows scatter plots depicting the significant positive correlation between MCM8 and the glycolysis genes ENO1, GAPDH, GPI, LDHA, and PGAM1 in three datasets (Fig. 6C, $P < 0.05$). These scatter plots provide a clear visualization of the relationship between MCM8 and the expression of key glycolysis genes in LUAD. We also identified 10 glycolysis-related genes in TCGA LUAD dataset

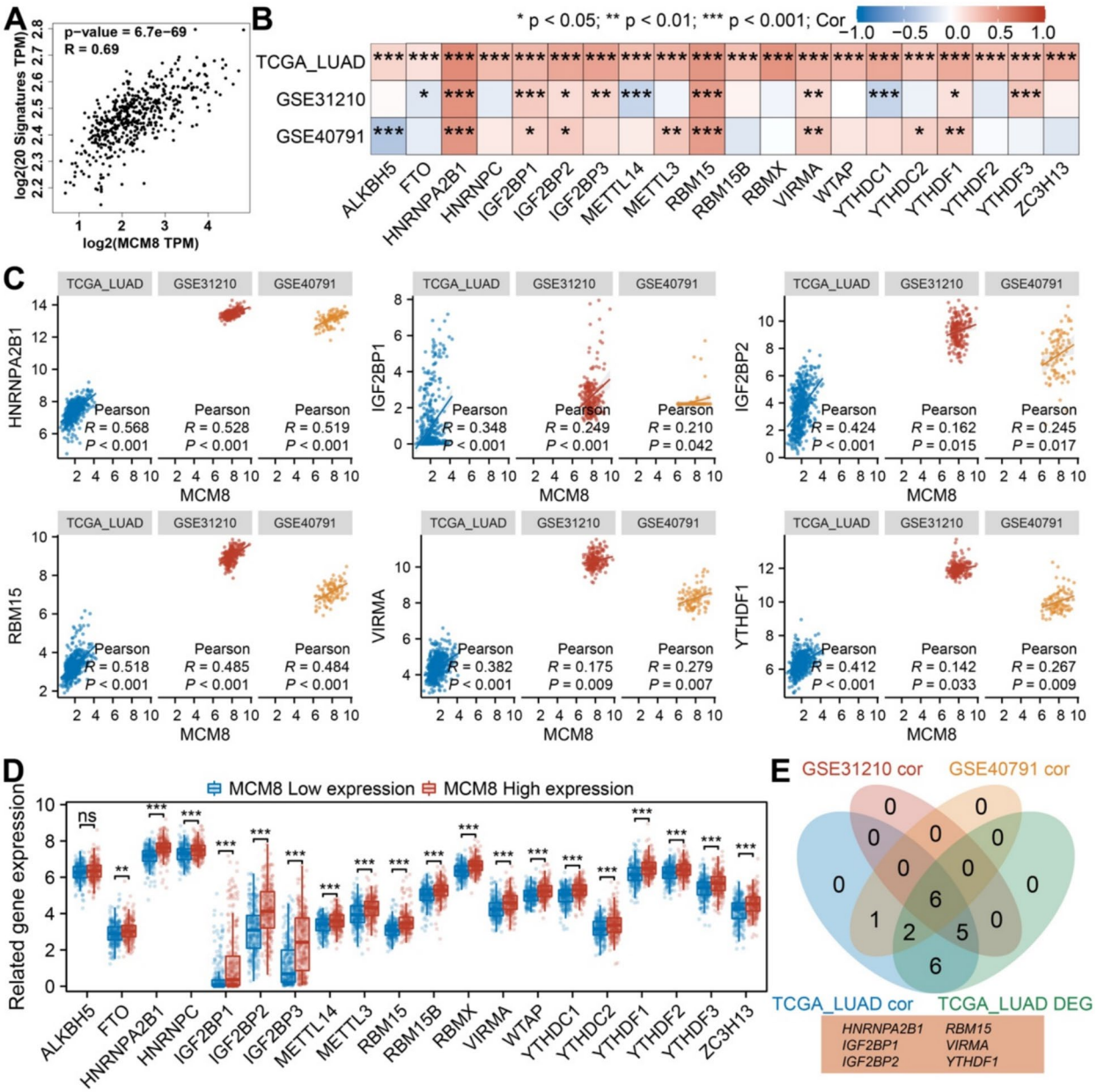

Fig. 5 Association Between MCM8 Expression and m6A Methylation Processes in LUAD. **A** Scatter plot showing a positive correlation between MCM8 expression and a selection of 20 m6A-related genes as evidenced by the GEPIA dataset. **B** Heatmap showing m6A genes positively and negatively associated with MCM8 from TCGA LUAD, GSE31210, and GSE40791 datasets. **C** Scatter plots showing significant positive correlations between MCM8 and six m6A genes (HNRNPA2B1, IGF2BP1, IGF2BP2, RBM15, VIRMA, and YTHDF1) in the three datasets. **D** Box plot shows 19 m6A differentially expressed genes between groups with high- and low-MCM8 expression groups in TCGA LUAD dataset. **E** Venn diagram illustrating the intersection of genes significantly related to MCM8 in the analyses, indicating potential connections with MCM8

that were significantly differentially expressed between high- and low-MCM8 expression groups, including SLC2A1, HK2, GPI, ALDOA, GAPDH, PGK1, PGAM1, ENO1, PKM, and LDHA (Fig. 6D, $P < 0.05$). This finding indicates that specific glycolysis-related genes may be regulated by MCM8 in LUAD cells. A Venn diagram showed that ENO1, GAPDH, GPI, LDHA, and PGAM1 met the criteria of all four analyses, suggesting a potential linkage with MCM8 (Fig. 6E). This overlap supports the hypothesis that MCM8 may play a role in regulating the glycolysis pathway in LUAD cells, specifically through its interaction with these five glycolysis genes. These

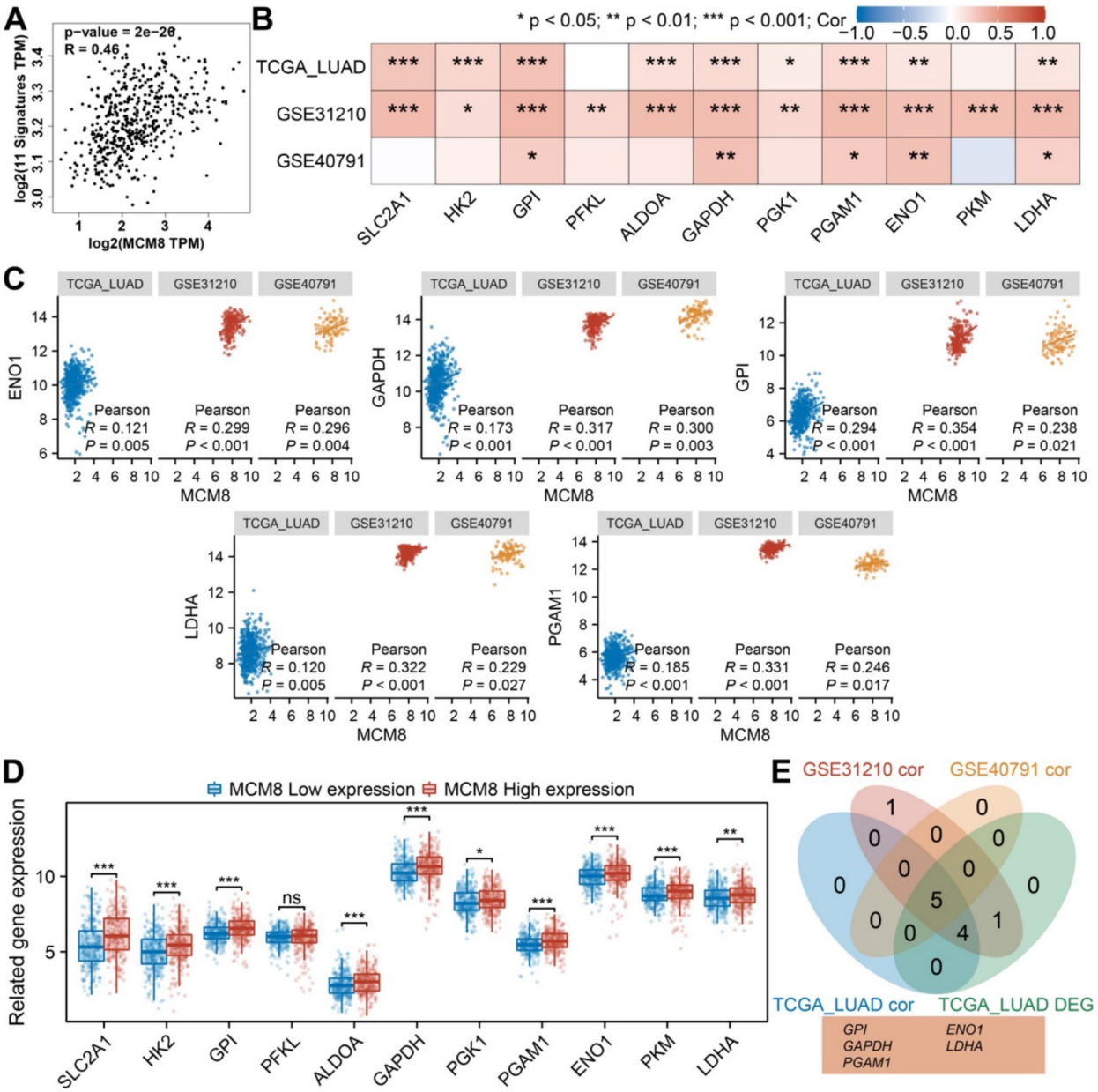

Fig. 6 Association between MCM8 Expression and the Glycolytic Pathway in Lung Adenocarcinoma (LUAD). **A** Correlation plot showing a positive association between MCM8 expression and 11 glycolysis-related genes identified in the GEPIA online platform LUAD dataset. **B** Heatmap showing a positive association between MCM8 and nine glycolysis-related genes (SLC2A1, HK2, GPI, ALDOA, GAPDH, PGK1, PGAM1, ENO1, and LDHA) in TCGA LUAD dataset and supporting correlations in two supplementary datasets, GSE31210 and GSE40791. **C** Scatter plots showing a significant positive correlation between MCM8 and five glycolysis-related genes (ENO1, GAPDH, GPI, LDHA, and PGAM1) in the three datasets. **D** Box plot showing the differences in expression of 10 glycolysis-related genes between high- and low-MCM8 expression groups in TCGA LUAD dataset. **E** Venn diagram showing the overlap of glycolytic genes in the four analyses, which identified ENO1, GAPDH, GPI, LDHA, and PGAM1 as candidate MCM8 regulatory genes in LUAD

findings provide a foundation for further investigation into the potential mechanisms underlying the association between MCM8 and glycolysis in LUAD.

Correlations between MCM8 expression and ferroptosis-related genes in LUAD

The GEPIA online tool was used to evaluate the association between MCM8 expression and ferroptosis-related genes in LUAD. We found positive correlations between

MCM8 expression and a group of 25 ferroptosis-related genes (Fig. 7A, R = 0.39, P = 2.6e-19). Further analysis of TCGA LUAD dataset confirmed this association, demonstrating a positive correlation between MCM8 and 15 ferroptosis genes, namely HSPA5, EMC2, SLC7A11, NFE2L2, MT1G, FANCD2, CISD1, SLC1A5, TFRC, LPCAT3, GLS2, CS, CARS, ATP5G3, and ACSL4, and a negative correlation with the expression of HSPB1, GPX4, RPL8, and DPP4 (Fig. 7B, P < 0.05). In the GSE31210 dataset, a notable positive correlation was observed between MCM8 expression and 9 ferroptosis-related genes, including HSPA5, SLC7A11, MT1G, FANCD2, CISD1, SLC1A5, CARS, ATP5G3, and AIFM2, and a significant negative correlation with FDFT1, SAT1, NCOA4, and ACSL4 (Fig. 7B, P < 0.05). In the GSE40791 dataset, MCM8 expression was significantly positively correlated with HSPA5, EMC2, SLC1A5, and ACSL4, and negatively correlated with CDKN1A (Fig. 7B, P < 0.05). Scatter plots show a significant positive correlation between MCM8 and the ferroptosis genes HSPA5 and SLC1A5 in the three datasets (Fig. 7C, P < 0.05). In TCGA LUAD dataset, 14 ferroptosis-related genes (HSPA5, EMC2, SLC7A11, NFE2L2, FANCD2, CISD1, SLC1A5, TFRC, LPCAT3, GLS2, CS, CARS1, ATP5MC3, and ACSL4) were significantly upregulated in the MCM8 high-expression group compared with the MCM8 low-expression group. GPX4 and RPL8 were expressed at higher levels in the MCM8 low-expression group (Fig. 7D, P < 0.05). Venn diagrams show that EHSPA5 and SLC1A5 met all four analysis criteria, indicating an association with MCM8 (Fig. 7E).

Discussion

LUAD is a prevalent subtype of non-small cell lung cancer and one of the leading causes of cancer-related mortality worldwide [1]. This malignancy poses significant health risks and negatively impacts quality of life due to

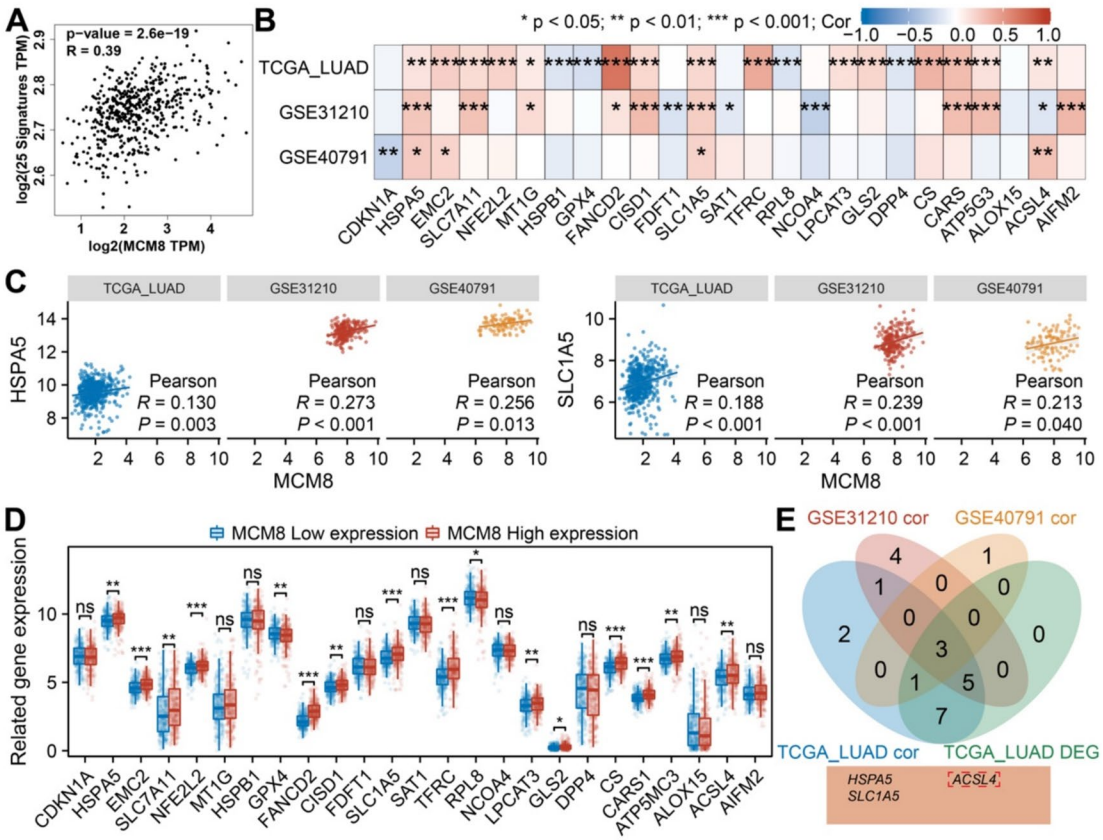

Fig. 7 Correlation of MCM8 Expression with Ferroptosis-related Genes in LUAD. **A** Significant positive correlations between MCM8 expression and 25 ferroptosis-related genes were observed. **B** MCM8 expression was positively correlated with 15 ferroptosis genes and negatively correlated with 4 ferroptosis genes in the TCGA LUAD dataset. Similar correlations were observed in the GSE31210 and GSE40791 datasets. **C** Scatter plots showing significant positive correlations between MCM8 and the ferroptosis genes HSPA5 and SLC1A5 in the three datasets. **D** Fourteen upregulated ferroptosis-related genes were identified in the MCM8 high-expression group compared with the low-expression group, whereas GPX4 and RPL8 were expressed at higher levels in the MCM8 low-expression group. **E** Venn diagrams showing that HSPA5 and SLC1A5 met all analysis criteria

its aggressive nature and challenges associated with its treatment [7, 36–38]. Early detection and diagnosis are critical, underscoring the need to identify reliable biomarkers and to elucidate the underlying molecular mechanisms to improve patient outcomes [6, 39–42].

The m6A modification is the most prevalent internal mRNA modification and plays a pivotal role in the progression of LUAD [43, 44]. Glycolysis, an essential metabolic process for tumor cell survival, has emerged as a therapeutic target in cancer, and its inhibition is considered a promising strategy [45, 46]. Ferroptosis, an iron-dependent form of programmed necrosis, plays a critical role in the initiation and progression of lung cancer [47]. Analysis of the expression patterns of genes such as MCM8 and their associations with immune cell infiltration and key biological processes may improve our understanding of the pathogenesis of LUAD. Understanding the association between genetic alterations, metabolic reprogramming, and immune microenvironment dynamics may lead to the design of personalized and effective therapeutic interventions for LUAD patients. The research mechanism is depicted in Fig. 8.

MCM8 is a member of the MCM family, which plays a crucial role in DNA replication and cell cycle progression. MCM8 co-immunoprecipitates with MCM6 and MCM7, forming a helicase complex essential for the initiation of DNA replication [48]. MCM8 expression is significantly higher in LUAD than in normal tissues, suggesting its potential role as a diagnostic biomarker. High MCM8 expression is associated with poor OS and DSS in LUAD patients, indicating its prognostic value [49]. Mechanistically, MCM8 is involved in the regulation of many biological processes, including cell cycle and DNA replication, which are critical for tumor progression [21, 22]. MCM8 is also involved in other cancers, such as glioma, where it promotes cancer cell growth and is associated with poor prognosis [50]. In gastric cancer (GC), MCM8 acts as a hub gene in circRNA-miRNA-mRNA regulatory networks, highlighting its central role in tumorigenesis [51]. MCM8 upregulation in GC is associated with shorter OS and progression-free survival, and knockdown of MCM8 inhibits cell growth, metastasis, and tumorigenesis, and induces apoptosis, supporting its role as a driver of tumor progression [18]. In pancreatic cancer, overexpression of MCM8 is independently associated with poor prognosis, and its expression is associated with markers of disease progression such as tumor invasion and lymph node metastasis, suggesting the potential of MCM8 as a prognostic biomarker and therapeutic target [20]. In colorectal cancer, MCM8 is upregulated in tumor tissues and significantly associated with tumor grade and patient survival, and knockdown of MCM8 inhibits cell growth and motility while promoting apoptosis, further supporting its carcinogenic effect [21]. MCM8 overexpression in cervical cancer is significantly associated with tumor stage and is involved in key pathways such as DNA replication and cell cycle regulation, demonstrating its potential as a diagnostic and prognostic biomarker [17]. In bladder cancer, MCM8 is similarly upregulated and associated with poor prognosis. Functional studies show that inhibiting MCM8 suppresses malignant phenotypes by modulating key signaling pathways such as Akt and MAPK9, suggesting its potential as a therapeutic target [16]. Taken together, these findings

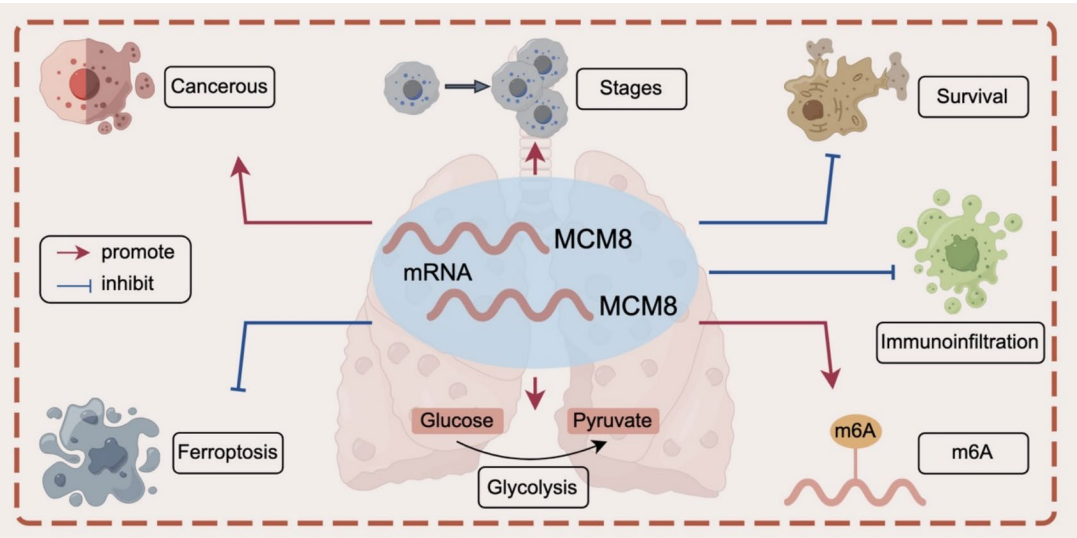

Fig. 8 Research mechanism diagram. The figure was created by Figdraw (http://www.figdraw.com)

suggest that MCM8 is involved in cancer progression and support its potential as a diagnostic and prognostic biomarker in many tumor types. Although the underlying mechanisms may vary according to tumor type, the consistent overexpression and association with poor outcomes highlight its clinical significance.

In this study, we identified several key pathways associated with MCM8 in LUAD. We found significant positive correlations between MCM8 and a set of m6A-related genes, including HNRNPA2B1, IGF2BP1, IGF2BP2, RBM15, VIRMA, and YTHDF1. These findings suggest a potential role for MCM8 in modulating m6A methylation during the development of LUAD. The roles of these m6A genes in LUAD progression were described previously. For instance, Liang et al. reported that HNRNPA2B1 suppresses SFRP2 through m6A-mediated miR-106b-5p maturation, thereby activating the Wnt/β-catenin pathway and exacerbating LUAD progression [52]. Liu et al. showed that IGF2BP1 is an independent predictor of the response to immune therapy in LUAD patients, and its expression is significantly associated with immune infiltration, immune checkpoint expression, and tumor mutational burden (TMB) [53]. Han et al. found that IGF2BP2 can activate endothelial cells, promoting angiogenesis and metastasis in LUAD [54]. Ma et al. reported that RBM15-mediated m6A modification decreases RASSF8 protein levels and promotes the invasiveness and migratory capacity of LUAD tumor cells [55]. Guo et al. found that KIAA1429 modulates the expression of ARHGAP30, thereby regulating the proliferation and metastasis of LUAD through the PI3K/AKT pathway [56]. Fan et al. revealed that YTHDF1 promotes the expression of DUSP5 and the malignant phenotype of LUAD cells [57]. These findings indicate that exploring the mechanisms underlying the regulation of MCM8 expression and its interplay with m6A modification during cancer progression is important.

We found a robust positive correlation between MCM8 and genes implicated in glycolysis, specifically ENO1, GAPDH, GPI, LDHA, and PGAM1. These glycolytic genes are involved in the progression of LUAD, underscoring their significance in the metabolic reprogramming characteristic of cancer cells [58–61]. The observed association between MCM8 and glycolysis-related genes suggests that MCM8 plays a role in the glycolytic pathway during LUAD progression. MCM8 may modulate the metabolic phenotype of LUAD cells, which may contribute to their glycolytic dependency, thereby affecting proliferative and invasive capabilities.

HSPA5, a member of the heat shock protein family, promotes LUAD cell migration and metastasis by activating the Gαq-Rho GTPase signaling pathway [62]. Zhang et al. demonstrated that TRIM6 decreases ferroptosis and chemotherapeutic sensitivity in lung cancer by targeting SLC1A5 [63]. We found a strong positive correlation between MCM8 and ferroptosis-associated genes, notably HSPA5 and SLC1A5, suggesting that MCM8 plays a role in modulating the ferroptosis pathway during LUAD progression. Elucidating the specific mechanisms underlying the involvement of MCM8 in ferroptosis could shed light on the role of ferroptosis in cancer progression and identify potential therapeutic targets for LUAD. These findings underscore the intricate interplay between MCM8 and pivotal pathways in LUAD, laying a solid foundation for further investigations into the pathogenesis of LUAD and the development of targeted therapeutic strategies.

The immune infiltration analysis revealed significant differences in immune cell types between high- and low-MCM8 expression groups in LUAD. The high-MCM8 expression group exhibited elevated levels of CD4 memory activated T cells and resting NK cells, as well as macrophages M0 and M1, whereas the low-MCM8 expression group showed higher infiltration of plasma cells, regulatory T cells (Tregs), activated NK cells, monocytes, resting dendritic cells, and resting mast cells. These findings are consistent with previous studies indicating that MCM8 expression is associated with immune cell infiltration in various cancers, including hepatocellular carcinoma and gliomas [22, 50]. The presence of different immune cell types in the tumor microenvironment (TME) is associated with cancer progression and may predict prognosis [64, 65]. CD4 memory activated T cells enhance antitumor immunity by supporting cytotoxic T lymphocyte (CTL) function, whereas macrophages M0 and M1 are involved in tumor promotion and suppression, respectively [66, 67]. On the other hand, regulatory T cells (Tregs) and monocytes in the low-MCM8 expression group are typically associated with immunosuppressive functions, which can facilitate tumor immune evasion [67]. The differential infiltration patterns observed in this study indicate that MCM8 may influence the TME by modulating the recruitment and activation of specific immune cell populations. This could have significant implications for the development of immunotherapeutic strategies targeting MCM8. For instance, the elevated infiltration of CD4 memory activated T cells and macrophages M1 in the high-MCM8 expression group may contribute to tumor progression, while the increased presence of Tregs and other immunosuppressive cells in the low-MCM8 expression group could be associated with a more suppressive tumor microenvironment in LUAD. The present findings highlight the potential of MCM8 as a biomarker for immune infiltration and its role in shaping the immune landscape of LUAD. Further research is warranted to elucidate the underlying

mechanisms and to explore the therapeutic potential of targeting MCM8 in combination with immunotherapies.

MCM8 shows significant promise as a biomarker for LUAD with both diagnostic and prognostic applications. Its overexpression in LUAD tissues, as demonstrated in this study, supports its potential for early detection, particularly in high-risk populations, as evidenced by the high diagnostic accuracy observed in the ROC analysis. Kaplan–Meier survival analysis revealed that MCM8 expression is associated with patient outcomes, suggesting its utility in stratifying patients into risk categories to inform personalized treatment strategies. Beyond these roles, the involvement of MCM8 in critical tumorigenic processes, such as DNA replication, repair, and immune modulation, underscores its potential as a therapeutic target. Targeting MCM8 could disrupt these essential pathways and enhance the efficacy of combination therapies, including immunotherapies and other targeted approaches. Additionally, the observed association between MCM8 expression and immune cell infiltration patterns highlights its potential as a biomarker for predicting response to immunomodulatory treatments. These findings collectively suggest that MCM8 could play a pivotal role in advancing precision oncology in LUAD.

Conclusion

In summary, this study demonstrated that MCM8 is expressed at higher levels in LUAD than in normal tissues, supporting its potential as a diagnostic and prognostic biomarker. We also found an association between MCM8 expression and immune cell infiltration, as well as its correlation with key biological processes such as m6A RNA methylation, glycolysis, and ferroptosis. These insights provide a foundation for further research into the role of MCM8 in LUAD and other cancers. Future studies should focus on validating these findings through experimental and clinical approaches, which could pave the way for the development of novel therapeutic strategies targeting MCM8 and its associated pathways.

Acknowledgements
We thank International Science Editing (http://www.internationalscienceediting.com) for editing this manuscript.

Author contributions
X.-S.L.: Conceptualization, Methodology, Writing—Original Draft. J.X.: Conceptualization, Software. R.-M.W.: Data Curation. G.-C.X.: Data Curation. Y.Z.: Software, Validation. Z.-J.P.: Supervision, Writing—Review & Editing.

Funding
This work was supported by the Hubei Provincial Natural Science Foundation of China (2024AFD284), Hubei Provincial Clinical Research Center for precision Diagnosis and Treatment of Liver Cancer Open Fund (2024LCOF08), Innovative Research Program for Graduates of Hubei University of Medicine (grant no. YC2024042), the Shiyan Taihe Hospital hospital-level project (2024JJXM087), and the Key Discipline Project of Hubei University of Medicine.

Availability of data and materials
The datasets presented in this study can be found in online repositories. The names of the repository/repositories and accession number(s) can be found in the Materials and Methods.

Declarations

Ethics approval and consent to participate
The studies involving human participants were reviewed and approved by Ethics Committee of Taihe Hospital Affiliated of Hubei University of Medicine (NO. 2024KS20), and was in accordance with the Declaration of Helsinki. Written informed consent for participation was not required for this study in accordance with the Ethics Committee of Taihe Hospital Affiliated with Hubei University of Medicine.

Competing interests
The authors declare no competing interests.

Received: 20 November 2024 Accepted: 25 February 2025
Published online: 03 March 2025

References

1. Siegel RL, Giaquinto AN, Jemal A. Cancer statistics, 2024. CA Cancer J Clin. 2024;74:12–49. https://doi.org/10.3322/caac.21820.
2. Sung H, Ferlay J, Siegel RL, Laversanne M, Soerjomataram I, Jemal A, Bray F. Global cancer statistics 2020: GLOBOCAN estimates of incidence and mortality worldwide for 36 cancers in 185 countries. CA Cancer J Clin. 2021;71:209–49. https://doi.org/10.3322/caac.21660.
3. Cao H, Xue Y, Wang F, Li G, Zhen Y, Guo J. Identification of prognostic molecular subtypes and model based on CD8+ T cells for lung adenocarcinoma. Biocell. 2024;48:473–90. https://doi.org/10.32604/biocell.2024.048946.
4. Zheng Y, Su Y, Ruan L, He Q, Gong L, Li J. Screening and biomarker assessment of ferroptosis genes *FLT3* and *ALOX5* in lung adenocarcinoma. Oncologie. 2023;25:281–9. https://doi.org/10.1515/oncologie-2023-0090.
5. Ullah A, Razzaq A, Alfaifi MY, Elbehairi SEI, Menaa F, Ullah N, Shehzadi S, Nawaz T, Iqbal H. Sanguinarine attenuates lung cancer progression via oxidative stress-induced cell apoptosis. Curr Mol Pharmacol. 2024;17:e18761429269383. https://doi.org/10.2174/0118761429269383231119062233.
6. Seguin L, Durandy M, Feral CC. Lung adenocarcinoma tumor origin: a guide for personalized medicine. Cancers. 2022;14:1759. https://doi.org/10.3390/cancers14071759.
7. Thai AA, Solomon BJ, Sequist LV, Gainor JF, Heist RS. Lung cancer. Lancet. 2021;398:535–54. https://doi.org/10.1016/S0140-6736(21)00312-3.
8. da Cunha Santos G, Shepherd FA, Tsao MSEGFR. Mutations and lung cancer. Annu Rev Pathol. 2011;6:49–69. https://doi.org/10.1146/annurev-pathol-011110-130206.
9. Leonetti A, Sharma S, Minari R, Perego P, Giovannetti E, Tiseo M. Resistance mechanisms to osimertinib in EGFR-mutated non-small cell lung cancer. Br J Cancer. 2019;121:725–37. https://doi.org/10.1038/s41416-019-0573-8.
10. Ozga AJ, Chow MT, Luster AD. Chemokines and the immune response to cancer. Immunity. 2021;54:859–74. https://doi.org/10.1016/j.immuni.2021.01.012.
11. Anichini A, Perotti VE, Sgambelluri F, Mortarini R. Immune escape mechanisms in non small cell lung cancer. Cancers. 2020;12:E3605. https://doi.org/10.3390/cancers12123605.
12. Santarpia M, Aguilar A, Chaib I, Cardona AF, Fancelli S, Laguia F, Bracht JWP, Cao P, Molina-Vila MA, Karachaliou N, et al. Non-small-cell lung cancer signaling pathways, metabolism, and PD-1/PD-L1 antibodies. Cancers. 2020;12:E1475. https://doi.org/10.3390/cancers12061475.
13. Liu X-S, Zhang Y, Ming X, Hu J, Chen X-L, Wang Y-L, Zhang Y-H, Gao Y, Pei Z-J. SPC25 as a novel therapeutic and prognostic biomarker and its association with glycolysis, ferroptosis and ceRNA in lung adenocarcinoma. Aging-us. 2024;16:779–98. https://doi.org/10.18632/aging.205418.

14. Liu X-S, Zhou L-M, Yuan L-L, Gao Y, Kui X-Y, Liu X-Y, Pei Z-J. NPM1 is a prognostic biomarker involved in immune infiltration of lung adenocarcinoma and associated with m6A modification and glycolysis. Front Immunol. 2021;12:724741. https://doi.org/10.3389/fimmu.2021.724741.
15. Yang L, Wang Q, He L, Sun X. The critical role of tumor microbiome in cancer immunotherapy. Cancer Biol Ther. 2024;25:2301801. https://doi.org/10.1080/15384047.2024.2301801.
16. Zhu W, Gao F, Zhou H, Jin K, Shao J, Xu Z. Knockdown of MCM8 inhibits development and progression of bladder cancer in vitro and in vivo. Cancer Cell Int. 2021;21:242. https://doi.org/10.1186/s12935-021-01948-2.
17. Wu B, Xi S. Bioinformatics analysis of the transcriptional expression of minichromosome maintenance proteins as potential indicators of survival in patients with cervical cancer. BMC Cancer. 2021;21:928. https://doi.org/10.1186/s12885-021-08674-y.
18. Huang B, Lin M, Lu L, Chen W, Tan J, Zhao J, Cao Z, Zhu X, Lin J. Identification of mini-chromosome maintenance 8 as a potential prognostic marker and its effects on proliferation and apoptosis in gastric cancer. J Cell Mol Medi. 2020;24:14415–25. https://doi.org/10.1111/jcmm.16062.
19. He D-M, Ren B-G, Liu S, Tan L-Z, Cieply K, Tseng G, Yu YP, Luo J-H. Oncogenic activity of amplified miniature chromosome maintenance 8 in human malignancies. Oncogene. 2017;36:3629–39. https://doi.org/10.1038/onc.2017.123.
20. Peng Y-P, Zhu Y, Yin L-D, Zhang J-J, Guo S, Fu Y, Miao Y, Wei J-S. The expression and prognostic roles of MCMs in pancreatic cancer. PLoS ONE. 2016;11: e0164150. https://doi.org/10.1371/journal.pone.0164150.
21. Yu S, Dai W, Zhao S, Yang Y, Xu Y, Wang J, Deng Q, He J, Shi D. Function and mechanism of MCM8 in the development and progression of colorectal cancer. J Transl Med. 2023;21:623. https://doi.org/10.1186/s12967-023-04084-9.
22. Yu M, Wang H, Xu H, Lv Y, Li Q. High MCM8 expression correlates with unfavorable prognosis and induces immune cell infiltration in hepatocellular carcinoma. Aging. 2022;14:10027–49. https://doi.org/10.18632/aging.204440.
23. Tomczak K, Czerwińska P, Wiznerowicz M. Review the cancer genome atlas (TCGA): an immeasurable source of knowledge. Współczesna Onkol. 2015;1A:68–77. https://doi.org/10.5114/wo.2014.47136.
24. Obuchowski NA, Bullen JA. Receiver operating characteristic (ROC) curves: review of methods with applications in diagnostic medicine. Phys Med Biol. 2018;63:07TR01. https://doi.org/10.1088/1361-6560/aab4b1.
25. Liu Z, Liu L, Weng S, Xu H, Xing Z, Ren Y, Ge X, Wang L, Guo C, Li L, et al. BEST: a web application for comprehensive biomarker exploration on large-scale data in solid tumors. J Big Data. 2023;10:165. https://doi.org/10.1186/s40537-023-00844-y.
26. Liu X-S, Chen Y-L, Chen Y-X, Wu R-M, Tan F, Wang Y-L, Liu Z-Y, Gao Y, Pei Z-J. Pan-cancer analysis reveals correlation between RAB3B expression and tumor heterogeneity, immune microenvironment, and prognosis in multiple cancers. Sci Rep. 2024;14:9881. https://doi.org/10.1038/s41598-024-60581-x.
27. Newman AM, Liu CL, Green MR, Gentles AJ, Feng W, Xu Y, Hoang CD, Diehn M, Alizadeh AA. Robust enumeration of cell subsets from tissue expression profiles. Nat Methods. 2015;12:453–7. https://doi.org/10.1038/nmeth.3337.
28. Chen B, Khodadoust MS, Liu CL, Newman AM, Alizadeh AA. Profiling tumor infiltrating immune cells with CIBERSORT. Methods Mol Biol. 2018;1711:243–59. https://doi.org/10.1007/978-1-4939-7493-1_12.
29. Tang Z, Li C, Kang B, Gao G, Li C, Zhang Z. GEPIA: a web server for cancer and normal gene expression profiling and interactive analyses. Nucleic Acids Res. 2017;45:W98–102. https://doi.org/10.1093/nar/gkx247.
30. Li Y, Xiao J, Bai J, Tian Y, Qu Y, Chen X, Wang Q, Li X, Zhang Y, Xu J. Molecular characterization and clinical relevance of m6A regulators across 33 cancer types. Mol Cancer. 2019;18:137–137. https://doi.org/10.1186/s12943-019-1066-3.
31. Lu C, Fang S, Weng Q, Lv X, Meng M, Zhu J, Zheng L, Hu Y, Gao Y, Wu X, et al. Integrated analysis reveals critical glycolytic regulators in hepatocellular carcinoma. Cell Commun Signaling. 2020;18:97. https://doi.org/10.1186/s12964-020-00539-4.
32. Li L, Liang Y, Kang L, Liu Y, Gao S, Chen S, Li Y, You W, Dong Q, Hong T, et al. Transcriptional regulation of the warburg effect in cancer by SIX1. Cancer Cell. 2018;33:368-385.e7. https://doi.org/10.1016/j.ccell.2018.01.010.
33. Liu Z, Zhao Q, Zuo Z-X, Yuan S-Q, Yu K, Zhang Q, Zhang X, Sheng H, Ju H-Q, Cheng H, et al. Systematic analysis of the aberrances and functional implications of ferroptosis in cancer. iScience. 2020;23:101302. https://doi.org/10.1016/j.isci.2020.101302.
34. Doll S, Freitas FP, Shah R, Aldrovandi M, Da Silva MC, Ingold I, Goya Grocin A, Xavier Da Silva TN, Panzilius E, Scheel CH, et al. FSP1 is a glutathione-independent ferroptosis suppressor. Nature. 2019;575:693–8. https://doi.org/10.1038/s41586-019-1707-0.
35. Liu X-S, Chen Y-X, Wan H-B, Wang Y-L, Wang Y-Y, Gao Y, Wu L-B, Pei Z-J. TRIP6 a potential diagnostic marker for colorectal cancer with glycolysis and immune infiltration association. Sci Rep. 2024;14:4042. https://doi.org/10.1038/s41598-024-54670-0.
36. Rudin CM, Brambilla E, Faivre-Finn C, Sage J. Small-cell lung cancer. Nat Rev Dis Prim. 2021;7:1–20. https://doi.org/10.1038/s41572-020-00235-0.
37. Herbst RS, Morgensztern D, Boshoff C. The biology and management of non-small cell lung cancer. Nature. 2018;553:446–54. https://doi.org/10.1038/nature25183.
38. Li Z, Li J, Bai X, Huang X, Wang Q. Tumor microenvironment as a complex milieu driving cancer progression: a mini review. Clin Transl Oncol. 2024. https://doi.org/10.1007/s12094-024-03697-w.
39. Tang Z, Wang L, Wu G, Qin L, Tan Y. FGD5 as a novel prognostic biomarker and its association with immune infiltrates in lung adenocarcinoma. Biocell. 2023;47:2503–16. https://doi.org/10.32604/biocell.2023.031565.
40. Mo B, Zhao X, Wang Y, Jiang X, Liu D, Cai H. Pan-cancer analysis, providing a reliable basis for IDO2 as a prognostic biomarker and target for immunotherapy. Oncologie. 2023;25:17–35. https://doi.org/10.1515/oncologie-2022-1026.
41. Wu Y, Lu S, Cheng Y, Zhou Q, Tu H, Zhou Q, Wang L, Zhang L, Zhou J, Huang C, et al. Uncommon/rare oncogenic drivers in non-small cell lung cancer: consensus and contention. Med Adv. 2023;1:293–305. https://doi.org/10.1002/med4.44.
42. Zhang J, Zhong W, Wu Y. Molecular residual disease: a new clue for individualized approach in non-small cell lung cancer. Med Adv. 2023;1:79–88. https://doi.org/10.1002/med4.11.
43. Yu M, Ji W, Yang X, Tian K, Ma X, Yu S, Chen L, Zhao X. The role of m6A demethylases in lung cancer: diagnostic and therapeutic implications. Front Immunol. 2023;14:1279735. https://doi.org/10.3389/fimmu.2023.1279735.
44. Teng P-C, Liang Y, Yarmishyn AA, Hsiao Y-J, Lin T-Y, Lin T-W, Teng Y-C, Yang Y-P, Wang M-L, Chien C-S, et al. RNA modifications and epigenetics in modulation of lung cancer and pulmonary diseases. Int J Mol Sci. 2021;22:10592. https://doi.org/10.3390/ijms221910592.
45. Smolle E, Leko P, Stacher-Priehse E, Brcic L, El-Heliebi A, Hofmann L, Quehenberger F, Hrzenjak A, Popper HH, Olschewski H, et al. Distribution and prognostic significance of gluconeogenesis and glycolysis in lung cancer. Mol Oncol. 2020;14:2853–67. https://doi.org/10.1002/1878-0261.12780.
46. Qiong L, Shuyao X, Shan X, Qian F, Jiaying T, Yao X, Hui L. Recent advances in the glycolytic processes linked to tumor metastasis. Curr Mol Pharmacol. 2024;17: e18761429308361. https://doi.org/10.2174/0118761429308361240823061634.
47. Zou J, Wang L, Tang H, Liu X, Peng F, Peng C. Ferroptosis in non-small cell lung cancer: progression and therapeutic potential on it. Int J Mol Sci. 2021;22:13335. https://doi.org/10.3390/ijms222413335.
48. Johnson EM. A new member of the mcm protein family encoded by the human mcm8 gene, located contrapodal to GCD10 at chromosome band 20p12.3–13. Nucleic Acids Res. 2003;31:2915–25. https://doi.org/10.1093/nar/gkg395.
49. Liu K, Kang M, Liao X, Wang R. Genome-wide investigation of the clinical significance and prospective molecular mechanism of minichromosome maintenance protein family genes in patients with lung adenocarcinoma. PLoS ONE. 2019;14: e0219467. https://doi.org/10.1371/journal.pone.0219467.
50. Yang S, Yuan Y, Ren W, Wang H, Zhao Z, Zhao H, Zhao Q, Chen X, Jiang X, Zhang L. MCM4 is a novel prognostic biomarker and promotes cancer cell growth in glioma. Front Oncol. 2022;12:1004324. https://doi.org/10.3389/fonc.2022.1004324.
51. Guan Y, Ma J, Song W. Identification of circRNA–miRNA–mRNA regulatory network in gastric cancer by analysis of microarray data. Cancer Cell Int. 2019;19:183. https://doi.org/10.1186/s12935-019-0905-z.
52. Rong L, Xu Y, Zhang K, Jin L, Liu X. HNRNPA2B1 Inhibited SFRP2 and activated Wnt-β/catenin via m6A-mediated miR-106b-5p processing to aggravate stemness in lung adenocarcinoma. Pathol Res Pract. 2022;233:153794. https://doi.org/10.1016/j.prp.2022.153794.

53. Liu J, Li Z, Cheang I, Li J, Zhou C. RNA-binding protein IGF2BP1 associated with prognosis and immunotherapy response in lung adenocarcinoma. Front Genet. 2022;13:777399. https://doi.org/10.3389/fgene.2022.777399.
54. Fang H, Sun Q, Zhou J, Zhang H, Song Q, Zhang H, Yu G, Guo Y, Huang C, Mou Y, et al. m6A methylation reader IGF2BP2 activates endothelial cells to promote angiogenesis and metastasis of lung adenocarcinoma. Mol Cancer. 2023;22:99. https://doi.org/10.1186/s12943-023-01791-1.
55. Ma M, Wang W, Li L, Wang X, Huang Q, Zhou C, Huang Y, Zhao G, Ye L. RBM15 facilities lung adenocarcinoma cell progression by regulating RASSF8 stability through N6 methyladenosine modification. Transl Oncol. 2024;46:102018. https://doi.org/10.1016/j.tranon.2024.102018.
56. Guo W, Wang T, Huai Q, Guo L, Wang X, He J. KIAA1429 regulates lung adenocarcinoma proliferation and metastasis through the PI3K/AKT pathway by modulating ARHGAP30 expression. Thorac Cancer. 2024;15:1397–409. https://doi.org/10.1111/1759-7714.15327.
57. Fan W, Xing Y, Yan S, Liu W, Ning J, Tian F, Wang X, Zhan Y, Luo L, Cao M, et al. DUSP5 regulated by YTHDF1-mediated m6A modification promotes epithelial-mesenchymal transition and EGFR-TKI resistance via the TGF-β/Smad signaling pathway in lung adenocarcinoma. Cancer Cell Int. 2024;24:208. https://doi.org/10.1186/s12935-024-03382-6.
58. Ma L, Xue X, Zhang X, Yu K, Xu X, Tian X, Miao Y, Meng F, Liu X, Guo S, et al. The essential roles of m6A RNA modification to stimulate ENO1-dependent glycolysis and tumorigenesis in lung adenocarcinoma. J Exp Clin Canc Res. 2022;41:36. https://doi.org/10.1186/s13046-021-02200-5.
59. Ouyang X, Zhu R, Lin L, Wang X, Zhuang Q, Hu D. GAPDH is a novel ferroptosis-related marker and correlates with immune microenvironment in lung adenocarcinoma. Metabolites. 2023;13:142. https://doi.org/10.3390/metabo13020142.
60. Han J, Deng X, Sun R, Luo M, Liang M, Gu B, Zhang T, Peng Z, Lu Y, Tian C, et al. GPI is a prognostic biomarker and correlates with immune infiltrates in lung adenocarcinoma. Front Oncol. 2021;11:752642. https://doi.org/10.3389/fonc.2021.752642.
61. Huang K, Liang Q, Zhou Y, Jiang L, Gu W, Luo M, Tang Y, Wang Y, Lu W, Huang M, et al. A novel allosteric inhibitor of phosphoglycerate mutase 1 suppresses growth and metastasis of non-small-cell lung cancer. Cell Metab. 2019;30:1107-1119.e8. https://doi.org/10.1016/j.cmet.2019.09.014.
62. Dong D-D, Zhou H, Li G. GPR78 promotes lung cancer cell migration and metastasis by activation of Gαq-Rho GTPase pathway. Bmb Rep. 2016;49:623–8. https://doi.org/10.5483/bmbrep.2016.49.11.133.
63. Zhang Y, Dong P, Liu N, Yang J-Y, Wang H-M, Geng Q. TRIM6 reduces ferroptosis and chemosensitivity by targeting SLC1A5 in lung cancer. Oxid Med Cell Longev. 2023;2023:9808100. https://doi.org/10.1155/2023/9808100.
64. Mao X, Xu J, Wang W, Liang C, Hua J, Liu J, Zhang B, Meng Q, Yu X, Shi S. Crosstalk between cancer-associated fibroblasts and immune cells in the tumor microenvironment: new findings and future perspectives. Mol Cancer. 2021;20:131. https://doi.org/10.1186/s12943-021-01428-1.
65. Cohen IJ, Pareja F, Socci ND, Shen R, Doane AS, Schwartz J, Khanin R, Morris EA, Sutton EJ, Blasberg RG. Increased tumor glycolysis is associated with decreased immune infiltration across human solid tumors. Front Immunol. 2022;13:880959. https://doi.org/10.3389/fimmu.2022.880959.
66. Wang P, Wang H, Huang Q, Peng C, Yao L, Chen H, Qiu Z, Wu Y, Wang L, Chen W. Exosomes from M1-polarized macrophages enhance paclitaxel antitumor activity by activating macrophages-mediated inflammation. Theranostics. 2019;9:1714–27. https://doi.org/10.7150/thno.30716.
67. Binnewies M, Mujal AM, Pollack JL, Combes AJ, Hardison EA, Barry KC, Tsui J, Ruhland MK, Kersten K, Abushawish MA, et al. Unleashing Type-2 dendritic cells to drive protective antitumor CD4+ T cell immunity. Cell. 2019;177:556-571.e16. https://doi.org/10.1016/j.cell.2019.02.005.

Publisher's Note